Action Potential Shortening and Impairment of Cardiac Function by Ablation of *Slc26a6*

See Editorial by Aiello et al

BACKGROUND: Intracellular pH (pH_i) is critical to cardiac excitation and contraction; uncompensated changes in pH_i impair cardiac function and trigger arrhythmia. Several ion transporters participate in cardiac pH_i regulation. Our previous studies identified several isoforms of a solute carrier Slc26a6 to be highly expressed in cardiomyocytes. We show that Slc26a6 mediates electrogenic Cl^-/HCO_3^- exchange activities in cardiomyocytes, suggesting the potential role of Slc26a6 in regulation of not only pH_i, but also cardiac excitability.

METHODS AND RESULTS: To test the mechanistic role of Slc26a6 in the heart, we took advantage of *Slc26a6* knockout (*Slc26a6*$^{-/-}$) mice using both in vivo and in vitro analyses. Consistent with our prediction of its electrogenic activities, ablation of *Slc26a6* results in action potential shortening. There are reduced Ca^{2+} transient and sarcoplasmic reticulum Ca^{2+} load, together with decreased sarcomere shortening in *Slc26a6*$^{-/-}$ cardiomyocytes. These abnormalities translate into reduced fractional shortening and cardiac contractility at the in vivo level. Additionally, pH_i is elevated in *Slc26a6*$^{-/-}$ cardiomyocytes with slower recovery kinetics from intracellular alkalization, consistent with the Cl^-/HCO_3^- exchange activities of Slc26a6. Moreover, *Slc26a6*$^{-/-}$ mice show evidence of sinus bradycardia and fragmented QRS complex, supporting the critical role of Slc26a6 in cardiac conduction system.

CONCLUSIONS: Our study provides mechanistic insights into Slc26a6, a unique cardiac electrogenic Cl^-/HCO_3^- transporter in ventricular myocytes, linking the critical roles of Slc26a6 in regulation of pH_i, excitability, and contractility. pH_i is a critical regulator of other membrane and contractile proteins. Future studies are needed to investigate possible changes in these proteins in *Slc26a6*$^{-/-}$ mice.

Padmini Sirish, PhD
Hannah A. Ledford, BA
Valeriy Timofeyev, PhD
Phung N. Thai, PhD
Lu Ren, MD
Hyo Jeong Kim, PhD†
Seojin Park, PhD
Jeong Han Lee, PhD
Gu Dai, PhD
Maryam Moshref, MS
Choong-Ryoul Sihn, PhD
Wei Chun Chen, PhD
Maria Valeryevna Timofeyeva, MS
Zhong Jian, PhD
Rafael Shimkunas, MS
Leighton T. Izu, PhD
Nipavan Chiamvimonvat, MD
Ye Chen-Izu, PhD
Ebenezer N. Yamoah, PhD
Xiao-Dong Zhang, PhD

†Deceased.

Correspondence to: Xiao-Dong Zhang, PhD, Division of Cardiovascular Medicine, Department of Internal Medicine, University of California, Davis, One Shields Ave, GBSF 6303, Davis, CA 95616. E-mail xdzhang@ucdavis.edu

Key Words: action potential ■ bradycardia ■ chloride-bicarbonate antiporters ■ myocardial contraction

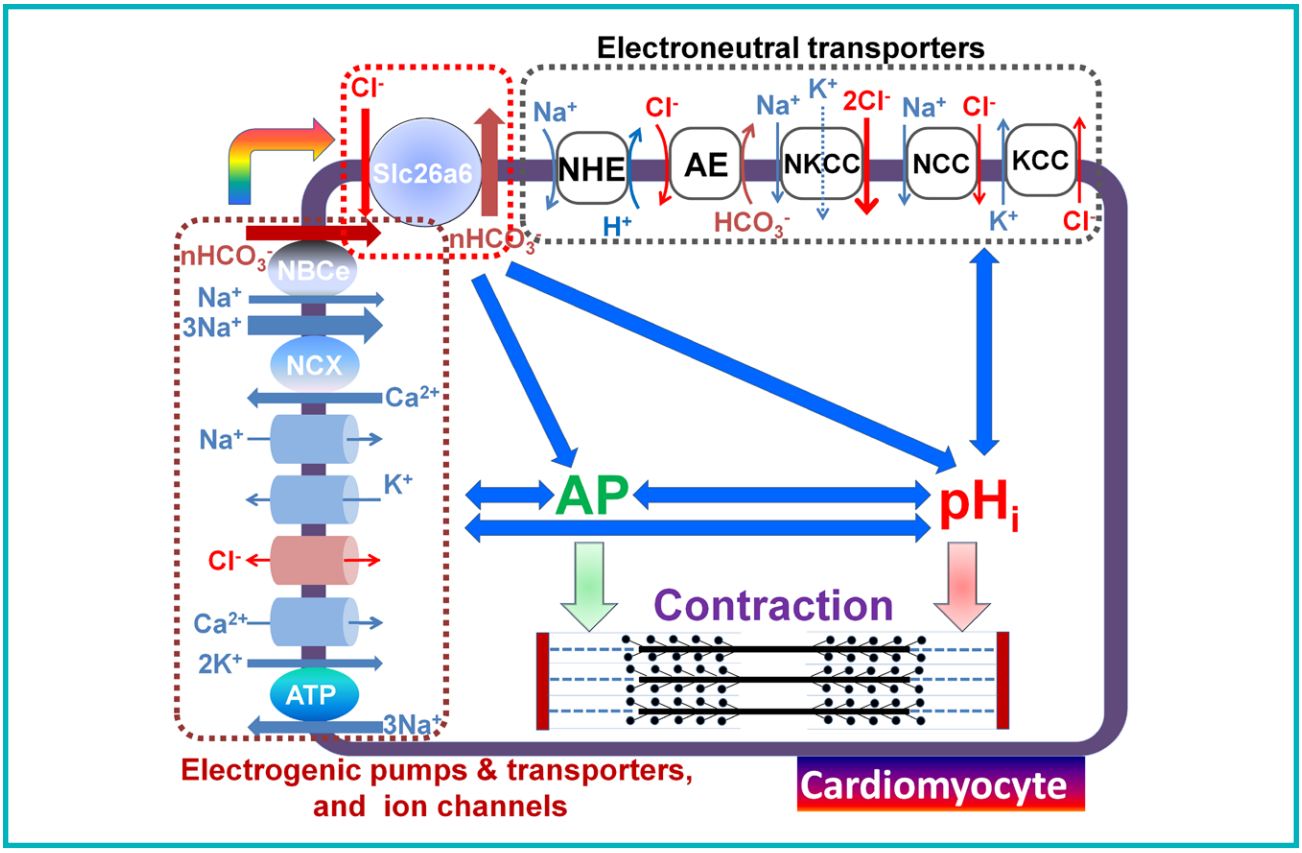

WHAT IS KNOWN?

- Intracellular pH (pH_i) is critical to cardiac excitation and contraction. Uncompensated changes in pH_i impair cardiac function and trigger arrhythmias; however, cardiac pH_i regulation mechanisms are not completely understood.
- Our previous studies identified several isoforms of a solute carrier, Slc26a6, to be highly expressed in mouse cardiomyocytes. We demonstrated that Slc26a6 mediates electrogenic Cl^-/HCO_3^- exchange activities in cardiomyocytes supporting the role of Slc26a6 in the regulation of pH_i and cardiac function.

WHAT THE STUDY ADDS?

- Ablation of *Slc26a6* resulted in action potential shortening, reduced Ca^{2+} transient and sarcoplasmic reticulum Ca^{2+} load, decreased sarcomere shortening, and elevated pH_i in mouse cardiomyocytes.
- At the in vivo level, *Slc26a6* knockout mice showed reduced fractional shortening and cardiac contractility, as well as fragmented QRS complexes, supporting the critical roles of Slc26a6 in the regulation of cardiac excitability and contractility.
- For the first time, we identified human cardiac SLC26A6 isoforms and demonstrated their electrogenic Cl^-/HCO_3^- exchange activities.

Acid–base balance is critical for maintaining normal cardiac function. An uncompensated shift of intracellular pH (pH_i) generates abnormal electrical activities, contractile disorder, and altered intracellular Ca^{2+} signaling.[1,2] The bicarbonate (HCO_3^-)/carbon dioxide (CO_2) buffering system plays a central role in regulation of pH_i. Therefore, transport of HCO_3^- across the plasma membrane is critical in maintaining cellular pH homeostasis. Several HCO_3^- transporters have been identified in cardiomyocytes, including Na^+/HCO_3^- cotransporter (NBC [sodium bicarbonate cotransporter]) and Cl^-/HCO_3^- exchanger (AE [anion] or CBE [chloride bicarbonate] exchangers).[1] NBC mediates acid extrusion, whereas AE mediates acid loading.

Solute carrier Slc26a6 is a versatile anion exchanger, first identified in epithelial cells, with abundant expression in kidneys, pancreas, intestines, and placenta.[3–5] It mediates Cl^-/oxalate, Cl^-/HCO_3^-, Cl^-/OH^-, Cl^-/SO_4^{2-}, and Cl^-/formate exchange activities. It was reported previously that Slc26a6 is the predominant Cl^-/HCO_3^- and Cl^-/OH^- exchanger in the mouse heart, based on the transcript levels.[6] Our recent functional study identified 4 cardiac Slc26a6 isoforms, which mediate Cl^-/HCO_3^- exchange in atrial and ventricular myocytes.[7] Importantly, we found that Cl^-/HCO_3^- exchange by cardiac Slc26a6 is electrogenic. Indeed, cardiac Slc26a6 represents the first electrogenic exchanger with only

anionic substrates and provides active transport of Cl^- into the cells to regulate intracellular Cl^- homeostasis. In addition, activities of Slc26a6 are predicted to alter the pH_i by transporting HCO_3^- or OH^-. Therefore, we hypothesize that cardiac Slc26a6 may play a unique role in the regulation of not only pH_i, but also cardiac excitability and function.

To directly test the hypothesis, we took advantage of a *Slc26a6* knockout (*Slc26a6*$^{-/-}$) mouse model[8] using in vivo and in vitro analyses. Under physiological conditions, Slc26a6 activities are predicted to coincide with the dynamic range of cardiac action potential (AP), generating mainly inward currents, with outward current beyond ≈+36 mV.[7] Indeed, our study reveals that ablation of *Slc26a6* results in AP shortening, consistent with electrogenic activities of Slc26a6. The shortened AP durations (APDs) result in reduced Ca^{2+} transient (CaT) and sarcoplasmic reticulum (SR) Ca^{2+} load, along with decreased sarcomere shortening in *Slc26a6*$^{-/-}$ cardiomyocytes. These abnormalities translate into reduced fractional shortening and cardiac contractility at the in vivo level. Importantly, pH_i is elevated in *Slc26a6*$^{-/-}$ cardiomyocytes with slower recovery kinetics from intracellular alkalization, consistent with Cl^-/HCO_3^- exchange activities of Slc26a6. Moreover, *Slc26a6*$^{-/-}$ mice show evidence of sinus bradycardia and fragmented QRS complex, supporting the critical role of Slc26a6 in cardiac conduction system.

MATERIALS AND METHODS

All animal care and procedures were performed in accordance with the protocols approved by Institutional Animal Care and Use Committee of the University of California, Davis, and in accordance with National Institutes of Health guidelines. De-identified human ventricular specimens were obtained from a commercial source, in accordance with the approved UC Davis Institutional Review Board protocol. Additional details are available in the Data Supplement.

We used 129S6/SvEv wild-type (WT) and *Slc26a6*$^{-/-}$ mice previously generated and reported[8] (a generous gift from Dr Peter S. Aronson, Yale University) in our study. All experiments described in the study were conducted in a blinded fashion.

Cardiac Tissue Preparation and Cardiomyocyte Isolation

Mice were anesthetized by IP injection of 80 mg/kg of ketamine and 5 mg/kg of xylazine. Cardiomyocytes were isolated as described previously.[7]

Genotyping, Western Blot, and Histological Analyses

Histological and Western blot analyses of cardiac tissue were performed as we have described previously.[9] Genotyping analyses of *Slc26a6*$^{-/-}$ mice are presented in Figure I in the Data Supplement.

Electrocardiographic Recordings

ECG recordings were performed as described previously.[10,11]

Analysis of Cardiac Function by Echocardiography

Echocardiograms to assess systolic function were performed in conscious animals as we have described previously.[10]

Hemodynamic Monitoring

Mice were anesthetized by IP injection of 80 mg/kg of ketamine and 5 mg/kg of xylazine and maintained at 37°C. Recording of pressure and volume was performed by using Millar Pressure-Volume System MPVS-300 (Millar, Inc, Houston, TX), Power Lab, and Lab Chart 6.0 software (AD Instruments, Colorado Springs, CO).

Patch-Clamp Recordings

Whole-cell current[7] and AP recordings[10] were performed as we have described previously. For current recordings, the clamped and suspended whole-cell was alternately exposed to theta capillary tubes dispensing control and test solutions at a potential of 0 mV.[7] For the outward current recording, we used the same solutions as we documented previously.[7]

For the inward current recording, the pipette solution contained (in mmol/L): 24 $NaHCO_3$, 116 Na glutamate, 1 EGTA, 1.4 NaCl, and gassed with 5% CO_2 and 95% O_2. The bath control solution was the same as the pipette solution. The bath test solution with 140 mmol/L Cl^- contained (in mmol/L): 140 NaCl, 10 HEPES, 1 EGTA, and pH 7.4; the bath test solution with 14 mmol/L Cl^- contained (in mmol/L): 14 NaCl, 126 Na glutamate, 10 HEPES, 1 EGTA, and pH 7.4. Current recordings were performed at the room temperature and APs were recorded at 36°C.

Measurement of Sarcomere Shortening and CaT

We used IonOptix sarcomere detection (IonOptix LLC, Westwood, MA) and the fast Fourier transform method.[12] Contraction was measured using a high-speed camera (MyoCam-S, 240–1000 frames/s) to record sarcomere movement. The sarcomere pattern was used to calculate the sarcomere length using a fast Fourier transform algorithm. The fractional shortening was calculated as the percentage change in sarcomere length during contraction. Simultaneous CaTs were recorded using Fura-2 dual-wavelength ratiometric method,[12] which is more precise than the Fluo-4 single-wavelength method.

The recording solution contained (in mol/L): 145 NaCl, 4 KCl, 1 $CaCl_2$, 0.33 NaH_2PO_4, 1 $MgCl_2$, 10 glucose, 10 HEPES, with pH 7.4. In a separate set of experiments, HCO_3^- was used as a buffer and the recording solution contained (in mmol/L): 120 NaCl, 4 KCl, 1 $CaCl_2$, 0.33 NaH_2PO_4, 1 $MgCl_2$, 10 glucose, 24 $NaHCO_3$, gassed by 5% CO_2, and 95% O_2. To reduce the pH_i, but keep extracellular pH (pH_o) constant, sodium acetate was applied to clamp the pH_i.[13,14] Sodium acetate was used to replace an equal concentration of NaCl, and 5 μmol/L 5-(*N*-ethyl-*N*-isopropyl) amiloride was added to inhibit the Na^+/H^+ exchanger for acetate application.

pH_i Measurement

The pH_i of cardiomyocytes was measured using carboxy-seminaphthorhodafluor-1 (carboxy-SNARF-1) fluorescent pH indicator. Isolated cardiomyocytes were loaded with 10 μmol/L SNARF-1 AM in Tyrode solution. The measurement was performed using Na^+-free solutions, buffered by either HEPES or HCO_3^-. HEPES-buffered solution contained (in mmol/L): 144 NMG-Cl, 4 KCl, 1 $MgCl_2$, 2 $CaCl_2$, 10 glucose, 10 HEPES, and pH 7.4. HCO_3^--buffered solution contained (in mmol/L): 120 NMG-Cl, 4 KCl, 1 $MgCl_2$, 2 $CaCl_2$, 10 glucose, 24 choline-HCO_3, gassed by 5% CO_2 and 95% O_2. Sodium acetate was used to clamp pH_i, and 5 μmol/L 5-(*N*-ethyl-*N*-isopropyl) amiloride was added to inhibit the Na^+/H^+ exchanger for acetate application.

The SNARF emission ratio (F_{580}/F_{640}) was converted to pH_i using standard calibration.[15–17] Calibration solutions with 5 different pH values were used. The calibration solutions contained (in mmol/L): 140 KCl, 1 $MgCl_2$, 20 HEPES (or MES [2-(*N*-morpholino) ethanesulfonic acid] at pH 5.5), with pH 5.5, 6.5, 7.0, 7.5, and 8.0. Nigericin (10 μmol/L, a K^+/H^+ antiporter ionophore) was added to the calibration solution before use.

Molecular Cloning From Human Cardiac Tissues

Deidentified human ventricular specimens were obtained from a commercial source, in accordance with the approved UC Davis Institutional Review Board protocol. Total RNA and mRNA were extracted, and similar cloning strategy was used as described previously.[7]

Heterologous Expression in Chinese Hamster Ovary Cells

Human cardiac SLC26A6 isoforms were expressed in Chinese hamster ovary cells following the protocol we used previously.[7]

Statistical Analyses

Data are presented as mean±SEM. Statistical comparisons were analyzed by Student *t* test. Statistical significance was considered to be achieved when $P<0.05$.

RESULTS

Ablation of *Slc26a6*$^{-/-}$ Results in Cardiac AP Shortening

To test the functional roles of Slc26a6, we took advantage of an *Slc26a6*$^{-/-}$ mouse model.[8] We first confirmed the lack of Slc26a6 expression in ventricular myocytes isolated from *Slc26a6*$^{-/-}$ mice (Figure 1A). The 2 bands observed in WT lane suggest the different mouse cardiac slc26a6 isoforms we reported previously.[7] To test the role of Slc26a6 in Cl^-/HCO_3^- and Cl^-/oxalate exchange, we recorded outward currents using fast solution exchange and suspended whole-cell recording methods, as we have described previously.[7] Figure 1B and 1C show the solution exchange configuration and corresponding currents, respectively, recorded from WT and *Slc26a6*$^{-/-}$ ventricular myocytes. The outward Cl^-/HCO_3^- and Cl^-/oxalate exchange currents were completely abolished in *Slc26a6*$^{-/-}$ ventricular myocytes (Figure 1C, right).

Because cardiac Slc26a6 is an electrogenic Cl^-/HCO_3^- exchanger, we predict that activities of Slc26a6 will affect cardiac APDs. There were no significant differences in the resting membrane potentials; however, APD at 90% repolarization (APD_{90}) was significantly shorter in *Slc26a6*$^{-/-}$ ventricular myocytes than in WT (Figure 1D through 1F). It has been reported previously that the stoichiometry of cardiac Slc26a6 for HCO_3^-:Cl^- is 2 or greater; therefore, the estimated reversal potential of the exchange is ≈+36 mV under physiological conditions. Our findings are consistent with the prediction that Slc26a6 generates inward currents by electrogenic Cl^-/HCO_3^- exchange through most of the AP, because of the positive reversal potential for Cl^-/HCO_3^- exchange under physiological conditions in cardiomyocytes.[7] Indeed, a prominent inward current can be generated in cardiomyocytes via Cl^-/HCO_3^- exchange with 24 mmol/L HCO_3^- inside the cells (Figure 1G).

APD shortening may also be caused by remodeling of other major ion channels such as Ca^{2+} and K^+ channels from knockout of *Slc26a6*. Therefore, we recorded Ca^{2+} and total K^+ currents from WT and *Slc26a6*$^{-/-}$ ventricular myocytes. As shown in Figure II in the Data Supplement, there were no significant differences in the current density between WT and *Slc26a6*$^{-/-}$ myocytes.

Slc26a6$^{-/-}$ Cardiomyocytes Show Reduced Sarcomere Shortening, CaT, and SR Ca^{2+} Load

The shortening of cardiac APs in *Slc26a6*$^{-/-}$ is predicted to result in decreased Ca^{2+} entry and possible impairment of cardiomyocyte contractility. We, therefore, tested CaT, sarcomere shortening, and SR Ca^{2+} load in WT and *Slc26a6*$^{-/-}$ ventricular myocytes using HEPES (Cl^-/OH^- exchange, Figure 2A through 2D) or HCO_3^- (Cl^-/HCO_3^- exchange, Figure 2E through 2H) buffered solutions. Compared with WT cardiomyocytes, *Slc26a6*$^{-/-}$ cardiomyocytes demonstrated significantly reduced fractional shortening and CaT amplitude (Figure 2A and 2B). To test whether the decrease in CaT resulted from reduced SR Ca^{2+} content, we measured the SR Ca^{2+} load in WT and *Slc26a6*$^{-/-}$ cardiomyocytes (Figure 2C and 2D). Indeed, the SR Ca^{2+} load was significantly reduced in *Slc26a6*$^{-/-}$ cardiomyocytes. Similar findings are shown for HCO_3^- buffered solution (Figure 2E through 2H).

Roles of Slc26a6 in pH_i Regulation

To test whether the Cl^-/HCO_3^- exchange, mediated by Slc26a6, contributes to pH_i regulation in ventricular myo-

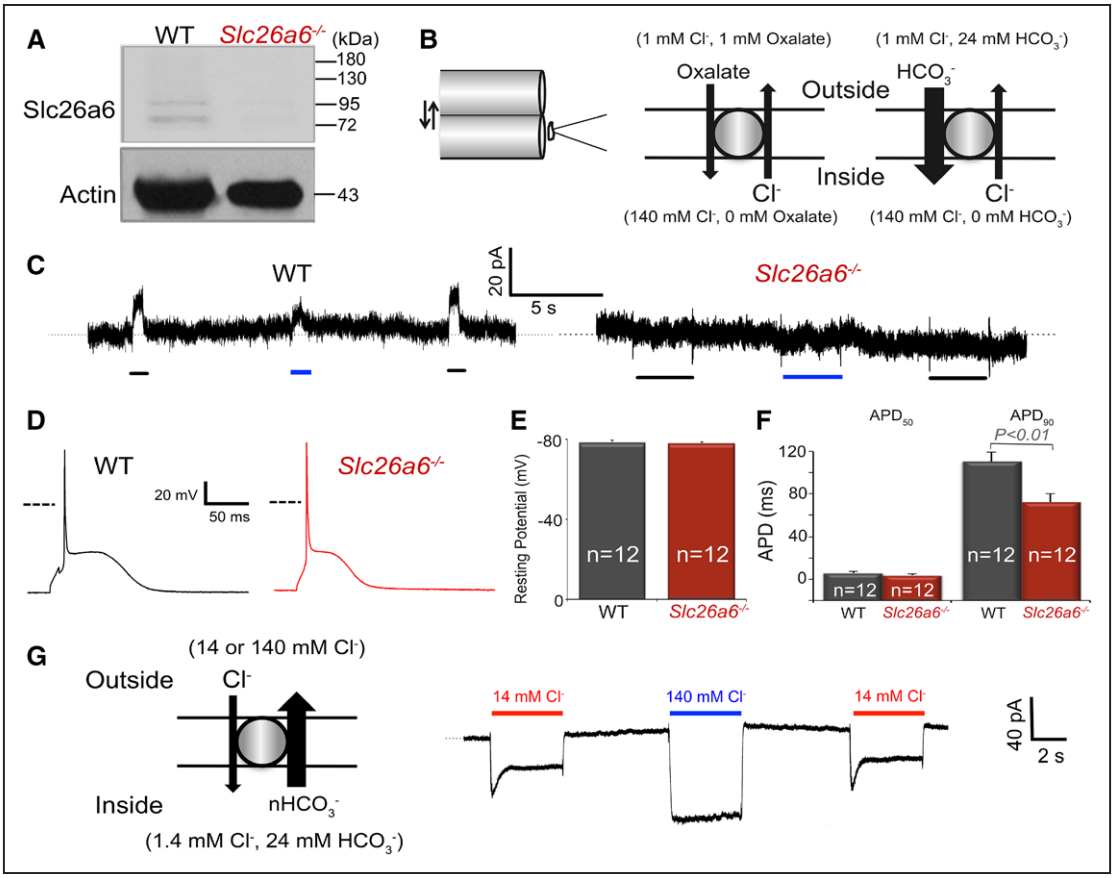

Figure 1. Ablation of *Slc26a6*$^{-/-}$ results in cardiac action potential shortening.
A, Western blot analysis confirms the absence of Slc26a6 expression in *Slc26a6*$^{-/-}$ mouse hearts. **B**, Schematic diagram of the fast solution exchange of the suspended whole-cell recording (**left**) and the ionic configuration to activate outward exchange current through Slc26a6. For recordings of the outward Slc26a6 currents, cardiomyocytes were first clamped at 0 mV, suspended, and moved to the outlet of the solution exchange capillary tube dispensing the bath control solution. Then the myocyte was switched to the capillary tube dispensing bath test solution, containing oxalate or HCO_3^-, for the activation of outward currents. The fast solution switch was performed by SF-77 solution exchanger controlled by pClamp10 software. The compositions of the bath control and test solutions have been described in Methods. **C**, Representative recording traces of outward currents recorded from wild-type (WT) ventricular myocytes (**left**) and *Slc26a6*$^{-/-}$ ventricular myocytes (**right**). The black and blue bars under the current traces represent the solution exchange to bath test solutions to activate Cl^-/Oxalate and Cl^-/HCO_3^- exchange currents, respectively. **D**, Representative traces of APs from WT and *Slc26a6*$^{-/-}$ ventricular myocytes. Dashed lines represent 0 mV. **E**, Comparisons of resting membrane potentials (RMPs). **F**, Summary data of the AP durations at 50% (APD_{50}) and 90% repolarization (APD_{90}). The AP and RMP were recorded in HCO_3^- buffered bath solution. **G**, Inward Cl^-/HCO_3^- exchange current elicited from WT ventricular myocytes using fast solution exchange, as indicated in the diagram on the **left**. The red and blue bars above the current traces represent the solution exchange to bath test solutions containing 14 or 140 mmol/L Cl^- to activate Cl^-/HCO_3^- exchange currents, respectively. Numbers within the bar graphs represent the sample sizes.

cytes, we directly measured the pH_i of cardiomyocytes using SNARF-1 AM pH dye, as shown in Figure 3A and 3B. The pH_i in resting *Slc26a6*$^{-/-}$ cardiomyocytes was 7.42±0.02, significantly higher than that of 7.16±0.02 in WT cardiomyocytes. To test the function of Slc26a6 in acid loading, we first induced intracellular acidification by washin of 40 mmol/L acetate followed by an immediate washout and monitored the pH_i recovery from alkalization. The pH_i in WT cardiomyocytes recovered to the baseline level over time (Figure 3C), whereas there was a delay in the recovery of pH_i in *Slc26a6*$^{-/-}$ cardiomyocytes, over the same period of time (Figure 3D). The results suggested an impairment of the acidification process in *Slc26a6*$^{-/-}$ cardiomyocytes and participation of Slc26a6 in the acid loading in cardiomyocytes.

We reason, based on its exchange activities, that Slc26a6 contributes to acid loading in cardiomyocytes under normal physiological conditions and that ablation of Slc26a6 may delay the acid-loading process and affect the sarcomere shortening and CaT. We perfused ventricular myocytes with a solution containing 40 mmol/L sodium acetate to acidify the cytosol and monitored the sarcomere shortening and CaT, as shown in Figure 3E. Acid loading resulted in marked reduction of sarcomere short-

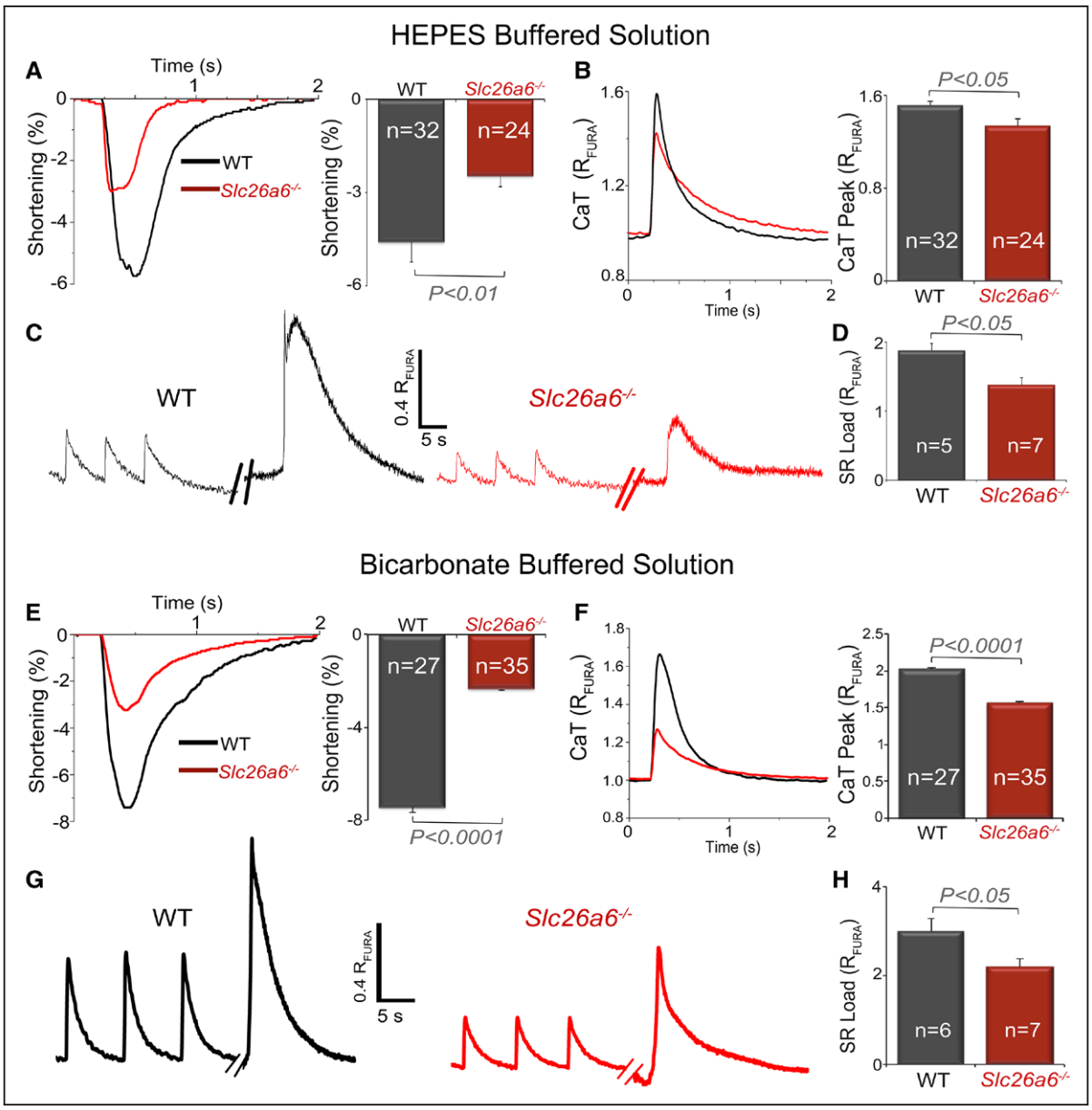

Figure 2. *Slc26a6*$^{-/-}$ cardiomyocytes show reduced sarcomere shortening, Ca^{2+} transient, and sarcoplasmic reticulum (SR) Ca^{2+} load.

Experiments were performed using HEPES (**A** through **D**) or HCO_3^- (**E** through **H**) as buffers. **A** and **E**, Representative traces and summary data for percentages of sarcomere shortening. **B** and **F**, Ca^{2+} transient (CaT) measured using Fura-2 ratio (R_{FURA}) from wild-type (WT) and *Slc26a6*$^{-/-}$ cardiomyocytes. **C** and **G**, Representative traces of SR Ca^{2+} load measurement of WT and *Slc26a6*$^{-/-}$ ventricular myocytes. The myocytes were first paced to steady state and then pacing was stopped for 15 s followed by a rapid application of 20 mmol/L caffeine to induce SR Ca^{2+} release. **D** and **H**, Summary data for SR Ca^{2+} load from WT and *Slc26a6*$^{-/-}$ ventricular myocytes. Numbers within the bar graphs represent the sample sizes.

ening in both WT and *Slc26a6*$^{-/-}$. The CaT was initially enhanced slightly and then inhibited by acetate-induced intracellular acidification. Moreover, after washout of acetate, the recovery process of sarcomere shortening and CaT was much slower in *Slc26a6*$^{-/-}$ cardiomyocytes, consistent with Slc26a6 exchange activities (note that different scales are used for upper and lower panels). The immediate alkalization during the washout of acetate also inhibited contraction of the cardiomyocytes.

Decrease in Fractional Shortening in *Slc26a6*$^{-/-}$ Mice

The above cellular data strongly support the contributions of Slc26a6 to cardiac pH_i, APD, and contractility. To test the effects of reduced CaT and sarcomere shortening in *Slc26a6*$^{-/-}$ on in vivo cardiac function, we performed echocardiography in conscious mice. There was no evidence of cardiac hypertrophy or dilation, with no significant

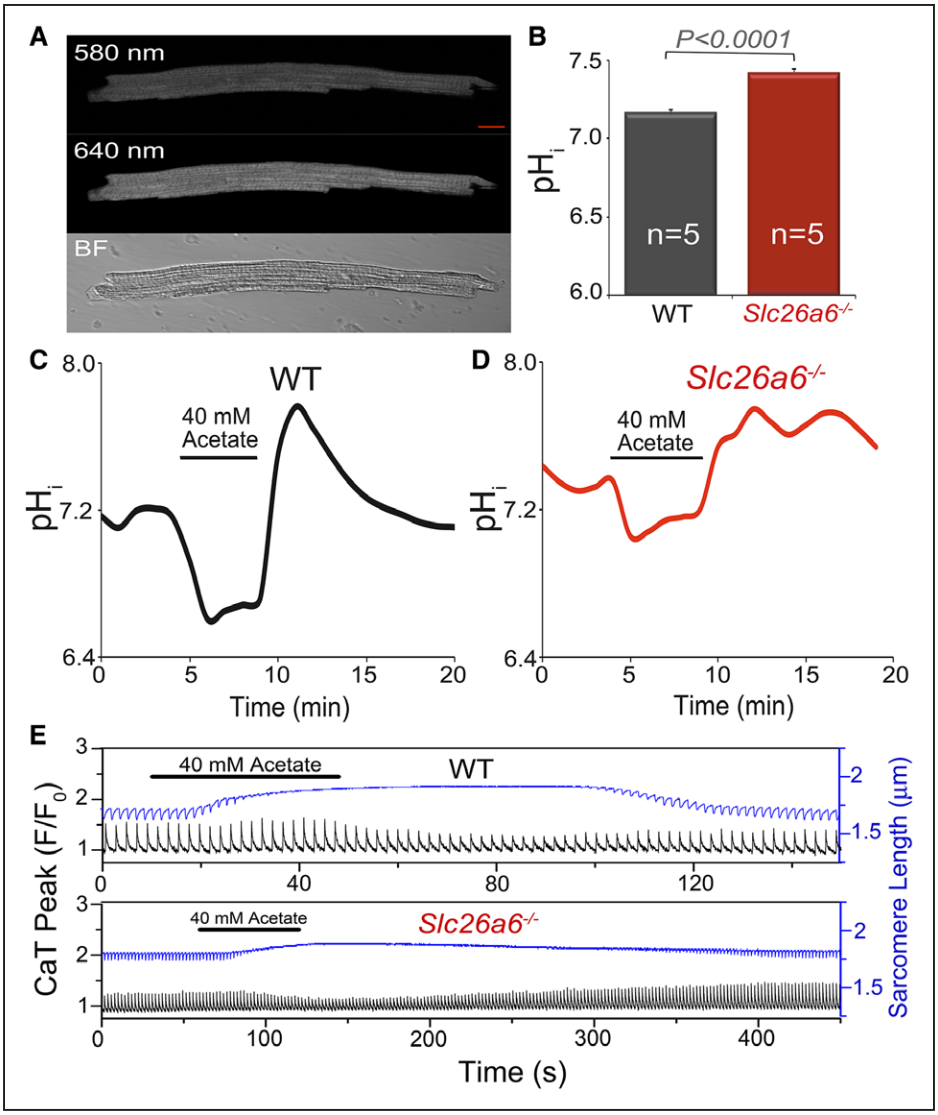

Figure 3. *Slc26a6*$^{-/-}$ cardiomyocytes show higher intracellular pH (pH$_i$).
A, Measurement of pH$_i$ in ventricular myocytes by seminaphthorhodafluor-1, acetoxymethyl ester (SNARF-1 AM) using confocal microscopy (scale bar=10 μm). Loaded cells were excited by 488-nm laser, and images were acquired by using 2 band-pass filters with center wavelengths of 580 and 640 nm, respectively. The ratio of the emission signals at 580 and 640 nm was calculated and converted to pH value following the standard methods described before.[15–17] A bright field (BF) image of the cardiomyocyte was also shown at the **lower** panel. **B**, Comparisons of pH$_i$ between wild-type (WT) and *Slc26a6*$^{-/-}$ cardiomyocytes. Alternations and recoveries of pH$_i$ when 40 mmol/L acetate was applied in WT (**C**) and *Slc26a6*$^{-/-}$ (**D**) ventricular myocytes. 5-(*N*-ethyl-*N*-isopropyl) amiloride (EIPA; 5 μmol/L) was added to inhibit the Na^+/H^+ exchanger during acetate application. **E**, Effects of 40 mmol/L acetate on CaT and sarcomere length in WT and *Slc26a6*$^{-/-}$ ventricular myocytes. EIPA (5 μmol/L) was added to inhibit the Na^+/H^+ exchanger during acetate application. The recovery process after washout of acetate for *Slc26a6*$^{-/-}$ myocytes is much slower than that of WT myocytes. The black traces showed the CaT, and the blue traces showed the sarcomere length. Numbers within the bar graphs represent the sample sizes.

differences in heart/body weight ratios between WT and *Slc26a6*$^{-/-}$ mice (Figure 4A and 4B). However, *Slc26a6*$^{-/-}$ mice showed evidence of sinus bradycardia (Figure 4C). Histological analyses, using wheat germ agglutinin and Picrosirius Red stain, of cardiac sections demonstrated no evidence of cardiac fibrosis, hypertrophy, or dilation in *Slc26a6*$^{-/-}$ mice (Figure 4D). However, there was a significant reduction in the fractional shortening in *Slc26a6*$^{-/-}$ mice compared with WT controls (Figure 4E).

Indeed, hemodynamic monitoring demonstrated a significant decrease in cardiac contractility in *Slc26a6*$^{-/-}$ mice compared with WT controls. Shown in Figure 5A are representative recordings of left ventricular pressure, volume, and developed pressure (dP/dt) in WT and *Slc26a6*$^{-/-}$ mice. There was a significant right and downward shift of the pressure–volume (P–V) loops in *Slc26a6*$^{-/-}$ mice, indicating reduced end-systolic pressure and relatively larger end-systolic and end-diastolic volumes, with reduced

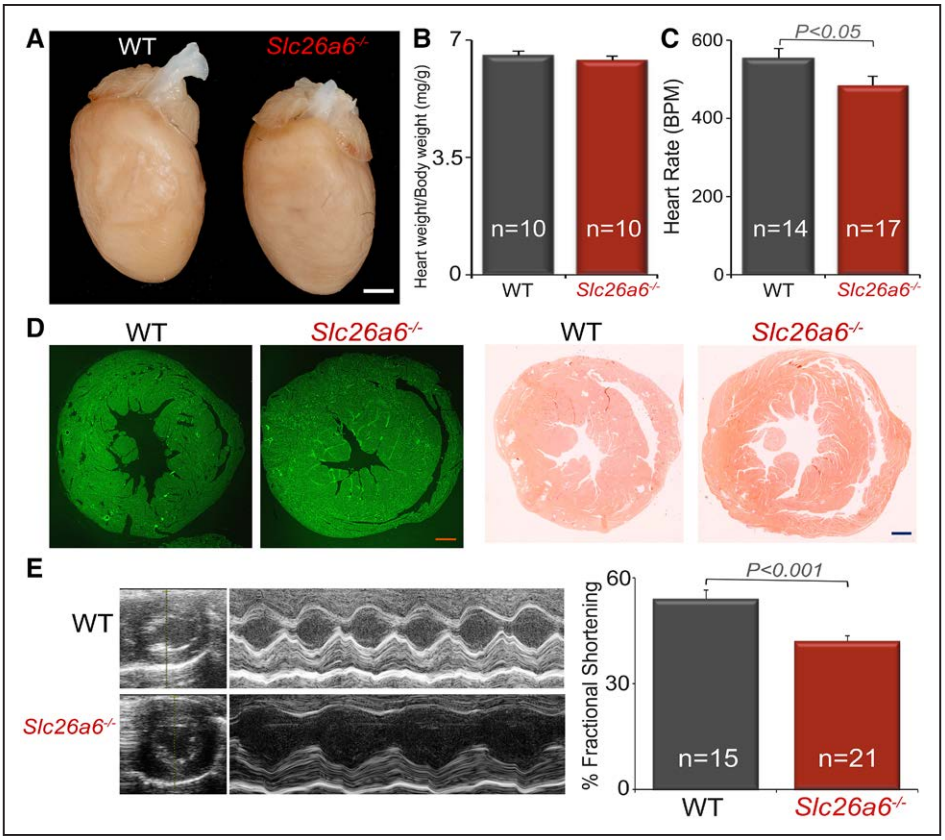

Figure 4. *Slc26a6*$^{-/-}$ mice demonstrate worsening fractional shortening and sinus bradycardia. **A**, Photomicrographs of whole heart of wild-type (WT) and *Slc26a6*$^{-/-}$ mice (scale bar=1 mm). **B**, Summary for heart/body weight ratio in mg/g. **C**, Heart rate. (BPM, beat per minute). **D**, Wheat germ agglutinin (**left** 2 panels) and Picrosirius Red (**right** 2 panels) staining of cardiac sections from WT and *Slc26a6*$^{-/-}$ mice demonstrating no evidence of increase fibrosis in the knockout mice (scale bar=0.5 mm). **E**, Two-dimensional and M-mode echocardiography from WT and *Slc26a6*$^{-/-}$ mice. The **right** panel shows summary data for fractional shortening (%FS), illustrating a significant decrease in %FS in knockout mice compared with WT. Numbers within the bar graphs represent the sample sizes.

stroke volume (Figure 5B). To determine the end-systolic P–V relationship, we obtained a series of P–V loops by altering the preload and derived the slope of the end-systolic P–V relationship (Ees), a load independent measure of cardiac contractility (Figure 5C and 5D for WT and *Slc26a6*$^{-/-}$, respectively). Consistent with the cellular and echocardiography data, the end-systolic pressure (Figure 5E), maximum dP/dt (Figure 5F), and Ees (Figure 5G) in *Slc26a6*$^{-/-}$ mice were significantly reduced when compared with those of WT mice, supporting a decrease in cardiac contractility in *Slc26a6*$^{-/-}$ mice.

Fragmented QRS Complex in *Slc26a6*$^{-/-}$ Mice

Cellular electrophysiology and pH_i measurement of *Slc26a6*$^{-/-}$ cardiomyocytes demonstrated the shortening of APD_{90} and elevated pH_i (Figures 1 and 3). We, therefore, compared the ECG between WT and *Slc26a6*$^{-/-}$ mice (Figure 6A and 6B). *Slc26a6*$^{-/-}$ mice showed evidence of fragmented QRS complex with prolonged PR interval. The QRS duration of *Slc26a6*$^{-/-}$ mice was significantly prolonged when compared with that of WT mice (22.8±0.8 ms versus 20.3±0.5 ms; n=8; $P<0.05$). Mice were challenged with subcutaneous isoproterenol (25 mg/kg; Figure 6C and 6D). Isoproterenol injection increased heart rates, but fragmented QRS complexes remained in *Slc26a6*$^{-/-}$ mice. Summary data are shown in Figure 6E and 6F. Of note, even though the heart rate measured by echocardiography was significantly reduced in unanesthesized *Slc26a6*$^{-/-}$ when compared with WT mice (Figure 4C), only the PR intervals were significantly prolonged in the anesthetized *Slc26a6*$^{-/-}$ mice during ECG recordings (Figure 6E). These in vivo findings suggest critical roles of Slc26a6 in cardiac conduction systems that warrant additional future investigations.

Molecular Identification of Human Cardiac SLC26A6 Isoforms

Previous studies suggest that Cl^-/oxalate exchange of mouse Slc26a6 is electrogenic, whereas the human SLC26A6 mediates electroneutral Cl^-/oxalate exchange.[18,19] To directly test whether there are indeed

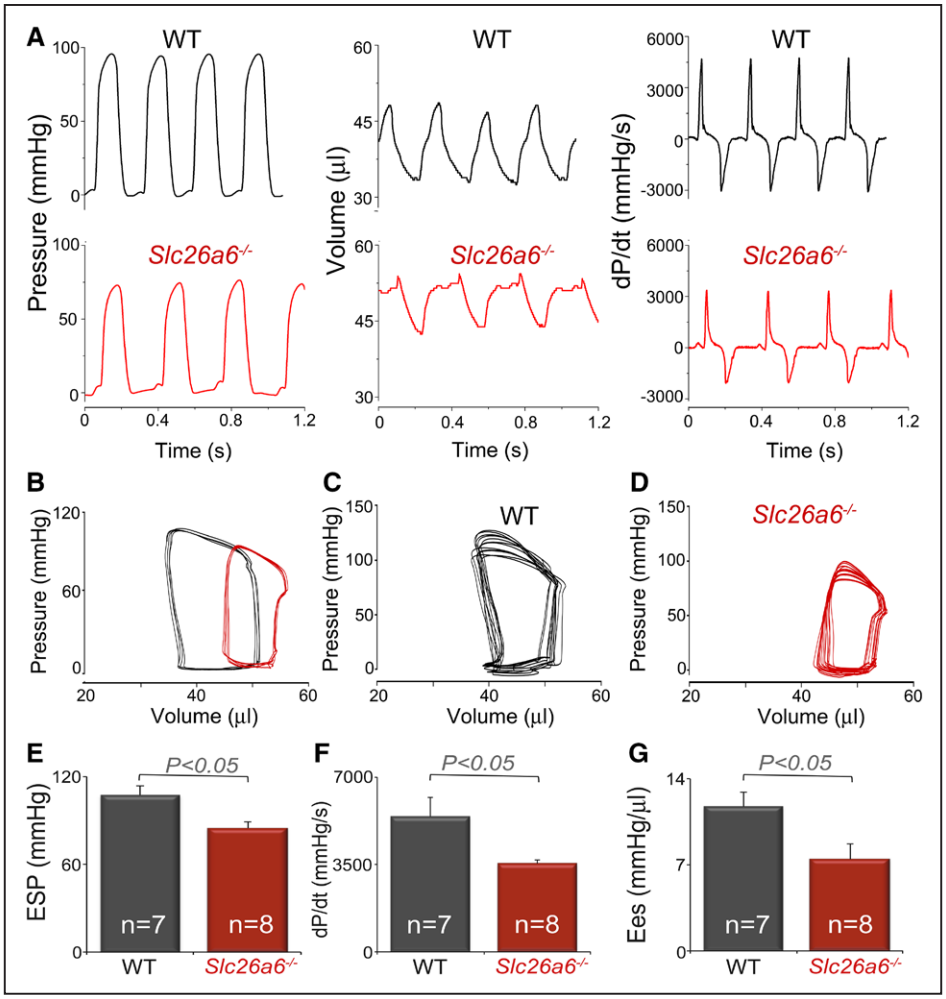

Figure 5. Hemodynamics monitoring from *Slc26a6*$^{-/-}$ and wild-type (WT) mice demonstrates the reduced cardiac contractility in *Slc26a6*$^{-/-}$ mice.

A, Recording traces of left ventricular pressure, volume, and derivative of pressure with respect to time (dP/dt) from WT and *Slc26a6*$^{-/-}$ mice. **B**, Pressure–Volume (P–V) loop analysis. The pressure and volume have been calibrated. The volume calibration was performed using cuvette (P/N 910–1049, Millar, Inc) filled with fresh heparinized 37°C mouse blood. A series of P–V loops when the preload was altered in WT (**C**) and *Slc26a6*$^{-/-}$ mice (**D**). **E** through **G**. Summary data for end-systolic pressure (ESP), maximum dP/dt, and the slope of the end-systolic P–V relationship (Ees). Numbers within the bar graphs represent the sample sizes.

species differences, we performed RT-PCR to clone full-length SLC26A6 from human heart (Figure 7).

Six different transcript variants of human SLC26A6 have been described previously. During the cloning of human cardiac SLC26A6, 2 major transcript variants were repetitively obtained, suggesting the presence of alternatively spliced variants of SLC26A6 in human heart. We used a For-long and Rev primer set, as well as a For-short and Rev primer set (Figure 7A); the PCR products are shown in Figure 7B. Twelve clones were randomly selected for each primer set, and the full-length sequence was confirmed by sequencing. Sequence analysis revealed that the 2 identified isoforms correspond to previously described transcript variant 2 (NM_134263.2) and transcript variant 4 (NM_001040454.1) for primer sets 1 and 2, respectively. Variant 4 is 21 amino acids shorter in the N terminus compared with transcript variant 2 (see protein sequence alignment in Figure III in the Data Supplement).

Electrogenic Cl^-/Oxalate and Cl^-/HCO_3^- Exchange Activities Mediated by Human Cardiac SLC26A6 Isoforms

To test the function of the human cardiac SLC26A6, we expressed the human cardiac SLC26A6 isoforms in Chinese hamster ovary cells and recorded the current generated by the anion exchanger, using patch-clamp coupled with a fast solution exchange technique, as described in Figure 1B and 1G. Membrane potential was held at 0 mV. Figure 7C shows the outward currents generated by electrogenic Cl^-/oxalate and Cl^-/

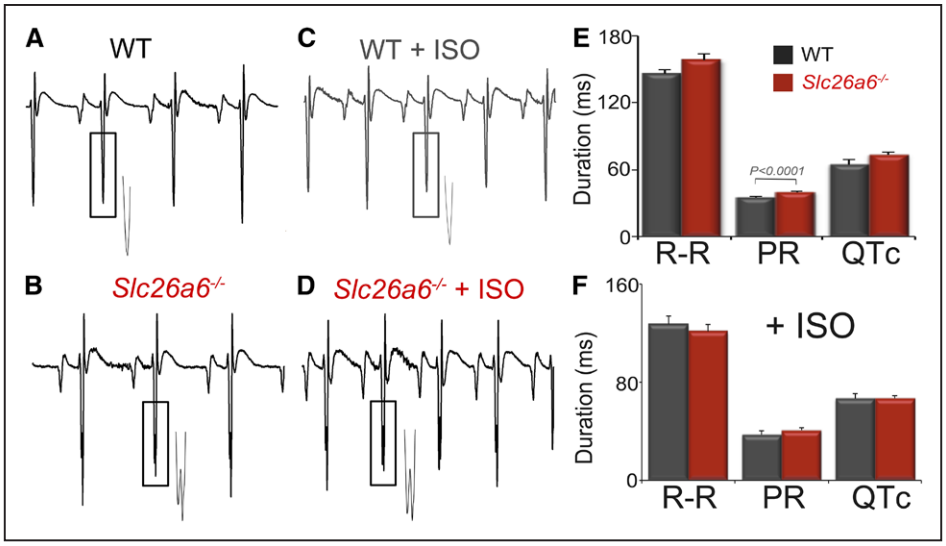

Figure 6. ECG recordings from age-matched wild-type (WT) and *Slc26a6*$^{-/-}$ mice reveal evidence of fragmented QRS complexes in the knockout mice.

A through **D**, Representative ECG traces. The insets showed the enlarged traces marked by the rectangular boxes demonstrating fragmented QRS complexes observed only in *Slc26a6*$^{-/-}$ mice. **E**, ECG parameters in control condition and with isoproterenol (ISO; **F**).

HCO_3^- exchanges and the inward currents generated by Cl^-/HCO_3^- exchanges. Both variants identified in human hearts are functional electrogenic Cl^-/oxalate and Cl^-/HCO_3^- exchangers.

DISCUSSION

Slc26a6 has been proposed to be the predominant Cl^-/HCO_3^- exchanger and a specific Cl^-/OH^- exchanger in the mouse heart, based on transcript levels.[6] Our group has since identified 4 cardiac Slc26a6 isoforms in the mouse heart, and importantly we demonstrated that mouse cardiac Slc26a6 mediates eletrogenic Cl^-/HCO_3^- exchange activities in cardiac myocytes.[7] We predict, based on its electrogenic activities, that Slc26a6 may participate not only in the regulation of pH_i, but also in cardiac excitability. To directly test this hypothesis, we took advantage of *Slc26a6*$^{-/-}$ mice. Consistent with our prediction, ablation of *Slc26a6* significantly shortens APD, resulting in reduced sarcomere shortening, CaT, and SR Ca^{2+} load, in addition to an elevated pH_i. Moreover, our in vivo studies demonstrate decreased fractional shortening and cardiac contractility, as well as sinus bradycardia in the knockout mice. Our results uncover new insights into the critical roles of cardiac electrogenic anion transporter—linking the regulation of not only pH_i, but also cardiac excitability and contractility.

Roles of Bicarbonate in Cardiac pH Regulation

HCO_3^-/CO_2 buffer is the major component of the cellular pH buffering system. Bicarbonate is the byproduct of mitochondrial respiration; therefore, its concentration is highly affected by physiological and pathological conditions. HCO_3^- is critical for pH regulation, acid/base secretion, and body fluid secretion.[20,21] Although CO_2 can diffuse across the plasma membrane, HCO_3^- transport across the plasma membrane requires facilitation by HCO_3^- transporters and anion channels. HCO_3^- transporters are encoded by 14 genes belonging to *SLC4A* and *SLC26A* gene families.[20]

The heart is an organ with a high metabolic rate, because of its continuous mechanical activities. Therefore, HCO_3^- is a critical anion in the regulation of cardiac function.[1,2] Unlike Na^+, K^+, and Ca^{2+} ions, which directly affect the excitability and contractility of the heart, HCO_3^- participates in the regulation of cardiac function through its coupled transport with other cations and anions, as well as its direct control of cardiac pH. Therefore, it is a unique anion in the heart with dynamic regulation and a wide range of function. HCO_3^- participates in acid extruding and acid-loading processes in cardiomyocytes, which are coupled with Na^+ and Cl^- transport, respectively.[1] Our studies provided strong evidence to support the role of Slc26a6 as an acid loader contributing to the acid-loading process in cardiomyocytes. Because cardiac Slc26a6 mediates Cl^-/HCO_3^- and Cl^-/OH^- exchange, our study also demonstrated the critical roles of Cl^- in regulation of cardiac function through Slc26a6.

Electrogenic Properties of Human SLC26A6

In contrast to our current findings, previous studies suggest that human SLC26A6 may not be electrogenic.[18,19] These studies, however, used an oocyte expression system and indirect measurement of changes in reversal

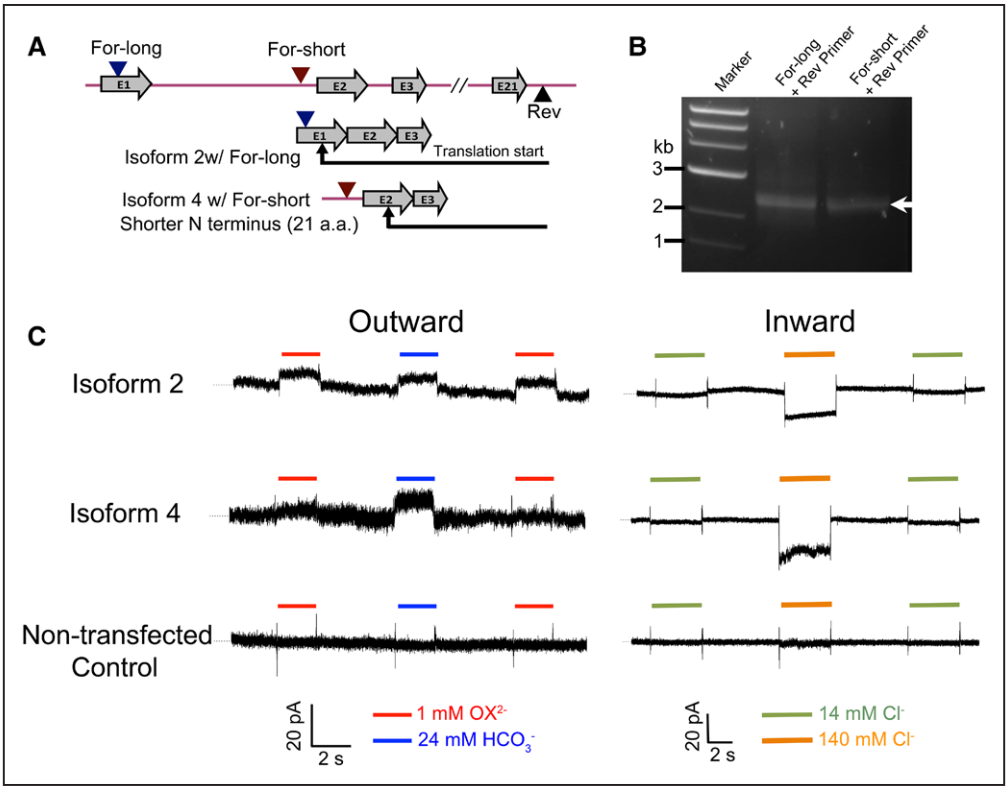

Figure 7. Molecular identification and functional analysis of human cardiac SLC26A6 isoforms.
A, The cloning strategy. Two different forward primers, For-long and For-short, were designed, corresponding to the genomic DNA sequence in chromosome 3 (NC_000003.12), one on 5′ untranslated region (5′-UTR) of exon 1 and the other on the intron sequence between exon 1 and exon 2, to verify isoforms having distinct 5′-UTR and 5′-end of coding sequence. The exon structure of the cloned isoforms is shown below. **B**, Reverse transcription–polymerase chain reaction (RT-PCR) amplification of the full-length cDNA of human cardiac SLC26A6 isoforms (indicated by an arrow) using 2 sets of primers. **C**, Patch-clamp recordings and fast solution exchange to activate 2 heterologously expressed human cardiac SLC26A6 isoforms that we have obtained. The outward current was activated by the solution exchange diagram shown in Figure 1B, and the inward current was activated by the solution exchange diagram shown in Figure 1G. Recordings on nontransfected Chinese hamster ovary cells are shown at the **bottom**. Dotted lines represent zero current.

potentials, wherein intracellular ion concentrations were unknown and could not be precisely controlled during the recordings. In contrast, we used patch-clamp recordings with fast solution exchange to precisely set the ionic gradient across the plasma membrane and monitor the dynamic changes of the currents. We observed electrogenic Cl^-/HCO_3^- and Cl^-/oxalate exchange activities of both mouse and human cardiac SLC26A6 (Figure 7).

Critical Roles of Electrogenic Transporters in Cardiac Excitability

Electrogenic transporters contribute significantly to cardiac excitability. The well-described Na^+/K^+ pump contributes to the generation of resting membrane potentials and repolarization of cardiac APs.[22] Another electrogenic transporter, Na^+/Ca^{2+} exchanger, is important not only in intracellular Ca^{2+} homeostasis and cardiac contractility, but also the regulation of cardiac excitability and arrhythmogenesis. Similar to *Slc26a6*$^{-/-}$, cardiac-specific Na^+/Ca^{2+} exchanger knockout mice show an abbreviated APD in cardiomyocytes.[23–25] Additionally, the electrogenic Na^+/HCO_3^- cotransporter was reported to modulate resting membrane potentials and cardiac APs.[26]

Slc26a6 mediates eletrogenic Cl^-/HCO_3^- exchange in the heart, thus regulating cardiac APD, as we demonstrate for the first time in this study. Based on the predicted stoichiometry of Slc26a6, at least 2 HCO_3^- are exchanged for 1 Cl^- ion, with estimated reversal potential of the exchange of ≈+36 mV. Under physiological conditions, the activation of Slc26a6 generates inward currents, which depolarize the membrane potential.[7] Consistently, *Slc26a6*$^{-/-}$ cardiomyocytes show shortened cardiac APs.

Functional Roles of Slc26a6 in Acid-Loading Process in Cardiomyocytes

The elevated pH_i in *Slc26a6*$^{-/-}$ cardiomyocytes supports the essential role of Slc26a6 in the acid-loading process.[1,2,6,7] Under physiological conditions, Slc26a6 mediates Cl^-/HCO_3^- or Cl^-/OH^- exchange, maintaining a relatively lower pH_i and higher intracellular Cl^- concen-

tration in cardiomyocytes. Here, we directly monitored the acidification process during the application and washout of acetate. *Slc26a6*$^{-/-}$ cardiomyocytes show delayed acidification, supporting the role of Slc26a6 in cellular acid loading (Figure 3).

In addition to Slc26a6, it has been reported that Slc4a families are expressed in cardiomyocytes, including AE1 (Slc4a1), AE2 (Slc4a2), and AE3 (Slc4a3), which are acid loaders. Other Slc4a members are mostly Na^+/HCO_3^- cotransporters, mediating acid extrusion.[1,6] However, the expression levels of AE1, AE2, AE3, and Slc26a3 are relatively low when compared with Slc26a6.[6] Nonetheless, it is possible that there is compensation from AE and other Slc26a families during the pH_i recovery process. The dominant molecule for acid loading is Slc26a6 because its expression level is nearly 100-fold higher than that of AEs and Slc26a3.

Decreased Cardiac Contractility in *Slc26a6*$^{-/-}$ Mice

The shortened cardiac APs are predicted to decrease Ca^{2+} influx through L-type Ca^{2+} channels, leading to reduced CaT and sarcomere fractional shortening in *Slc26a6*$^{-/-}$cardiomyocytes. Additionally, the elevated pH_i may contribute to changes in CaT and contractility. Indeed, pH_i is a critical regulator of cardiac ion channels and transporters, as well as other membrane and contractile proteins and, therefore, exerts significant influences on cardiac Ca^{2+} signaling, contractility, and excitability.[1,2] Effects of acidosis on cardiac function have been extensively investigated because of its pathological significance during ischemia-reperfusion.[27–34] Cellular acidification reduces CaT and contraction in cardiomyocytes.[1,27,29,31,35] Our results showed that CaT was initially enhanced and later inhibited by cellular acidification, induced by washin of acetate (Figure 3E) when Na^+/H^+ exchanger was inhibited, similar to that observed by Vaughan-Jones et al.[1] The reduced sarcomere shortening observed in our study from acidification (Figure 3E) agrees with previously reported findings.

On the other hand, effects of intracellular alkalization on cardiac contractility and CaT are less understood. Our findings in Figure 3E demonstrate that acid loading had a relatively small influence on CaT compared with cell shortening in both WT and *Slc26a6*$^{-/-}$ myocytes, however, alkalization during washout dramatically decreased CaT and cell shortening. The findings suggest that lower pH_i had a minor effect on CaT but may affect the Ca^{2+} affinity of troponin C.[1] Taken together, the impairment of cardiac contractility in *Slc26a6*$^{-/-}$ mice is likely due to multiple mechanisms, including alterations in pH_i, in addition to reduced APDs, CaT, and SR Ca^{2+} load.

Future Studies

One previous study using a different strain of *Slc26a6*$^{-/-}$ mice reported normal body weight, heart rate, and blood pressure in *Slc26a6*$^{-/-}$ mice.[36] Our studies demonstrate comparable heart/body weight ratio between WT and *Slc26a6*$^{-/-}$ mice; however, there is evidence of sinus bradycardia and fragmented QRS complex in *Slc26a6*$^{-/-}$ mice with prolonged PR interval. Fragmented QRS complexes have been shown to be common in patients post–myocardial infarction; they may represent a marker for cardiovascular diseases[37–39] and predict arrhythmic events and mortality in patients with cardiomyopathy.[40,41] Fragmented QRS was also reported to be prognostically significant in patients with Brugada syndrome, supporting the association of fragmented QRS and arrhythmia substrate.[42] *Slc26a6*$^{-/-}$ mice showed sinus bradycardia and fragmented QRS; however, there is no significant cardiac fibrosis in *Slc26a6*$^{-/-}$ mice. Our findings of fragmented QRS complexes and prolonged PR interval in *Slc26a6*$^{-/-}$ mice support the critical role of Slc26a6 not only in ventricular myocytes, but also in the cardiac conduction system. Sinus bradycardia in *Slc26a6*$^{-/-}$ mice further suggests functional roles of Slc26a6 in pacemaking cells.

In addition, the elevated pH_i may result in changes in gene expression profiles, as well as the function of other membrane and cytosolic proteins. For example, pH_i may affect APDs of rabbit and guinea pig ventricular myocytes by H^+-induced changes in late Ca^{2+} entry through the L-type Ca^{2+} channel.[43] Therefore, we expect a spectrum of cellular proteins that need to be further evaluated. However, these extensive investigations will be performed in our future experiments.

The global knockout of *Slc26a6* was reported to affect the kidney and duodenum epithelial transport[36] and induce Ca^{2+} oxalate urolithiasis.[8] The alteration in metabolic profiles in *Slc26a6*$^{-/-}$ may affect the observed in vivo cardiac function. Therefore, we took advantage of not only in vivo physiological measurement, but also in vitro analyses in our studies to circumvent these possible confounding factors. Indeed, our in vivo findings are consistent with in vitro analyses.

In conclusion, the current study unravels novel mechanistic insights into the newly described and unique cardiac electrogenic Cl^-/HCO_3^- transporter in ventricular myocytes. Activities of Slc26a6 contribute to not only the regulation of pH_i, but also cardiac AP and contractility. Ablation of *Slc26a6* shortens the APDs, impairs cardiac function, and results in fragmented QRS complexes and elevated pH_i. Additional studies are required to further understand the functional roles of Slc26a6 not only in ventricular myocytes, but also in pacemaking cells and the cardiac conduction system.

AFFILIATIONS

From the Division of Cardiovascular Medicine, Department of Internal Medicine (P.S., H.A.L., V.T., P.N.T., L.R., S.P., G.D., M.M., C.-R.S., W.C.C., M.V.T., N.C., Y.C.-I., X.-D.Z.), Center for Neuroscience (H.J.K.), Department of Pharmacology (Z.J., R.S., L.T.I., N.C., Y.C.-I.) and Department of Biomedical Engineering (R.S., Y.C.-I.), University of California, Davis; Department of Physiology and Cell Biology, School of Medicine, University of Nevada, Reno (J.H.L., E.N.Y.); and Department of Veterans Affairs, Northern California Health Care System, Mather (M.V.T., N.C., X.-D.Z.).

ACKNOWLEDGMENTS

We thank Dr Peter S. Aronson (Yale University) for his kind gift of *Slc26a6* knockout mice and reading of our article.

SOURCES OF FUNDING

This study was supported, in part, by American Heart Association Beginning Grant-in-Aid 14BGIA18870087 (Dr Zhang), National Institutes of Health (NIH) R01 DC015135, NIH R01 DC015252, NIH R01 DC016099, and NIH P01 AG051443 (Dr Yamoah), NIH R01 HL123526 (Dr Chen-Izu), NIH R01 HL085727, NIH R01 HL085844, NIH R01 HL137228, and S10 RR033106 (Dr Chiamvimonvat), VA Merit Review Grant I01 BX000576 and I01 CX001490 (Dr Chiamvimonvat), and American Heart Association Postdoctoral Fellowship Award (Dr Sirish). Dr Sirish received Postdoctoral Fellowship from California Institute for Regenerative Medicine Training Grant to UC Davis and NIH/National Heart, Lung and Blood Institute (NHLBI) Institutional Training Grant in Basic and Translational Cardiovascular Science (T32 NIH HL086350). H.A. Ledford and R. Shimkunas received Predoctoral Fellowship from NIH/NHLBI Institutional Training Grant in Basic and Translational Cardiovascular Science (T32 NIH HL086350) and NIH F31 Predoctoral Awards. M. Moshref received Predoctoral Fellowship from the Training Core of the NIH/National Institute of Environmental Health Sciences (NIEHS) UC Davis Superfund Program (P42 NIH ES004699). Dr Chiamvimonvat is the holder of the Roger Tatarian Endowed Professorship in Cardiovascular Medicine, University of California, Davis and a Staff Cardiologist, VA Medical Center, Mather, CA.

DISCLOSURES

None.

FOOTNOTES

Received March 26, 2017; accepted August 23, 2017.

The Data Supplement is available at http://circep.ahajournals.org/lookup/suppl/doi:10.1161/CIRCEP.117.005267/-/DC1.

Circ Arrhythm Electrophysiol is available at http://circep.ahajournals.org.

REFERENCES

1. Vaughan-Jones RD, Spitzer KW, Swietach P. Intracellular pH regulation in heart. *J Mol Cell Cardiol*. 2009;46:318–331. doi: 10.1016/j.yjmcc.2008.10.024.
2. Wang HS, Chen Y, Vairamani K, Shull GE. Critical role of bicarbonate and bicarbonate transporters in cardiac function. *World J Biol Chem*. 2014;5:334–345. doi: 10.4331/wjbc.v5.i3.334.
3. Mount DB, Romero MF. The SLC26 gene family of multifunctional anion exchangers. *Pflugers Arch*. 2004;447:710–721. doi: 10.1007/s00424-003-1090-3.
4. Dorwart MR, Shcheynikov N, Yang D, Muallem S. The solute carrier 26 family of proteins in epithelial ion transport. *Physiology (Bethesda)*. 2008;23:104–114. doi: 10.1152/physiol.00037.2007.
5. Alper SL, Sharma AK. The SLC26 gene family of anion transporters and channels. *Mol Aspects Med*. 2013;34:494–515. doi: 10.1016/j.mam.2012.07.009.
6. Alvarez BV, Kieller DM, Quon AL, Markovich D, Casey JR. Slc26a6: a cardiac chloride-hydroxyl exchanger and predominant chloride-bicarbonate exchanger of the mouse heart. *J Physiol*. 2004;561(pt 3):721–734. doi: 10.1113/jphysiol.2004.077339.
7. Kim HJ, Myers R, Sihn CR, Rafizadeh S, Zhang XD. Slc26a6 functions as an electrogenic Cl^-/HCO_3^- exchanger in cardiac myocytes. *Cardiovasc Res*. 2013;100:383–391. doi: 10.1093/cvr/cvt195.
8. Jiang Z, Asplin JR, Evan AP, Rajendran VM, Velazquez H, Nottoli TP, Binder HJ, Aronson PS. Calcium oxalate urolithiasis in mice lacking anion transporter Slc26a6. *Nat Genet*. 2006;38:474–478. doi: 10.1038/ng1762.
9. Sirish P, Li N, Timofeyev V, Zhang XD, Wang L, Yang J, Lee KS, Bettaieb A, Ma SM, Lee JH, Su D, Lau VC, Myers RE, Lieu DK, Lopez JE, Young JN, Yamoah EN, Haj F, Ripplinger CM, Hammock BD, Chiamvimonvat N. Molecular mechanisms and new treatment paradigm for atrial fibrillation. *Circ Arrhythm Electrophysiol*. 2016;9. doi: 10.1161/CIRCEP.115.003721.
10. Zhang XD, Timofeyev V, Li N, Myers RE, Zhang DM, Singapuri A, Lau VC, Bond CT, Adelman J, Lieu DK, Chiamvimonvat N. Critical roles of a small conductance Ca^{2+}-activated K^+ channel (SK3) in the repolarization process of atrial myocytes. *Cardiovasc Res*. 2014;101:317–325. doi: 10.1093/cvr/cvt262.
11. Mitchell GF, Jeron A, Koren G. Measurement of heart rate and Q-T interval in the conscious mouse. *Am J Physiol*. 1998;274(3 pt 2):H747–H751.
12. Jian Z, Han H, Zhang T, Puglisi J, Izu LT, Shaw JA, Onofiok E, Erickson JR, Chen YJ, Horvath B, Shimkunas R, Xiao W, Li Y, Pan T, Chan J, Banyasz T, Tardiff JC, Chiamvimonvat N, Bers DM, Lam KS, Chen-Izu Y. Mechanochemotransduction during cardiomyocyte contraction is mediated by localized nitric oxide signaling. *Sci Signal*. 2014;7:ra27. doi: 10.1126/scisignal.2005046.
13. Thomas RC. Experimental displacement of intracellular pH and the mechanism of its subsequent recovery. *J Physiol*. 1984;354:3P–22P.
14. Roos A, Boron WF. Intracellular pH. *Physiol Rev*. 1981;61:296–434.
15. Buckler KJ, Vaughan-Jones RD. Application of a new pH-sensitive fluoroprobe (carboxy-SNARF-1) for intracellular pH measurement in small, isolated cells. *Pflugers Arch*. 1990;417:234–239.
16. Blank PS, Silverman HS, Chung OY, Hogue BA, Stern MD, Hansford RG, Lakatta EG, Capogrossi MC. Cytosolic pH measurements in single cardiac myocytes using carboxy-seminaphthorhodafluor-1. *Am J Physiol*. 1992;263(1 pt 2):H276–H284.
17. Niederer SA, Swietach P, Wilson DA, Smith NP, Vaughan-Jones RD. Measuring and modeling chloride-hydroxyl exchange in the Guinea-pig ventricular myocyte. *Biophys J*. 2008;94:2385–2403. doi: 10.1529/biophysj.107.118885.
18. Chernova MN, Jiang L, Friedman DJ, Darman RB, Lohi H, Kere J, Vandorpe DH, Alper SL. Functional comparison of mouse slc26a6 anion exchanger with human SLC26A6 polypeptide variants: differences in anion selectivity, regulation, and electrogenicity. *J Biol Chem*. 2005;280:8564–8580. doi: 10.1074/jbc.M411703200.
19. Clark JS, Vandorpe DH, Chernova MN, Heneghan JF, Stewart AK, Alper SL. Species differences in Cl^- affinity and in electrogenicity of SLC26A6-mediated oxalate/Cl^- exchange correlate with the distinct human and mouse susceptibilities to nephrolithiasis. *J Physiol*. 2008;586:1291–1306. doi: 10.1113/jphysiol.2007.143222.
20. Cordat E, Casey JR. Bicarbonate transport in cell physiology and disease. *Biochem J*. 2009;417:423–439. doi: 10.1042/BJ20081634.
21. Casey JR, Grinstein S, Orlowski J. Sensors and regulators of intracellular pH. *Nat Rev Mol Cell Biol*. 2010;11:50–61. doi: 10.1038/nrm2820.

22. Bueno-Orovio A, Sánchez C, Pueyo E, Rodriguez B. Na/K pump regulation of cardiac repolarization: insights from a systems biology approach. *Pflugers Arch*. 2014;466:183–193. doi: 10.1007/s00424-013-1293-1.
23. Pott C, Henderson SA, Goldhaber JI, Philipson KD. Na^+/Ca^{2+} exchanger knockout mice: plasticity of cardiac excitation-contraction coupling. *Ann N Y Acad Sci*. 2007;1099:270–275. doi: 10.1196/annals.1387.015.
24. Pott C, Ren X, Tran DX, Yang MJ, Henderson S, Jordan MC, Roos KP, Garfinkel A, Philipson KD, Goldhaber JI. Mechanism of shortened action potential duration in Na^+-Ca^{2+} exchanger knockout mice. *Am J Physiol Cell Physiol*. 2007;292:C968–C973. doi: 10.1152/ajpcell.00177.2006.
25. Pott C, Philipson KD, Goldhaber JI. Excitation-contraction coupling in Na^+/Ca^{2+} exchanger knockout mice: reduced transsarcolemmal Ca^{2+} flux. *Circ Res*. 2005;97:1288–1295. doi: 10.1161/01.RES.0000196563.84231.21.
26. Villa-Abrille MC, Petroff MG, Aiello EA. The electrogenic Na^+/HCO_3^- cotransport modulates resting membrane potential and action potential duration in cat ventricular myocytes. *J Physiol*. 2007;578(pt 3):819–829. doi: 10.1113/jphysiol.2006.120170.
27. Bountra C, Vaughan-Jones RD. Effect of intracellular and extracellular pH on contraction in isolated, mammalian cardiac muscle. *J Physiol*. 1989;418:163–187.
28. Vaughan-Jones RD, Wu ML, Bountra C. Sodium-hydrogen exchange and its role in controlling contractility during acidosis in cardiac muscle. *Mol Cell Biochem*. 1989;89:157–162.
29. Orchard CH, Kentish JC. Effects of changes of pH on the contractile function of cardiac muscle. *Am J Physiol*. 1990;258(6 pt 1):C967–C981.
30. Harrison SM, Frampton JE, McCall E, Boyett MR, Orchard CH. Contraction and intracellular Ca^{2+}, Na^+, and H^+ during acidosis in rat ventricular myocytes. *Am J Physiol*. 1992;262(2 pt 1):C348–C357.
31. Fabiato A, Fabiato F. Effects of pH on the myofilaments and the sarcoplasmic reticulum of skinned cells from cardiace and skeletal muscles. *J Physiol*. 1978;276:233–255.
32. Steenbergen C, Deleeuw G, Rich T, Williamson JR. Effects of acidosis and ischemia on contractility and intracellular pH of rat heart. *Circ Res*. 1977;41:849–858.
33. Garlick PB, Radda GK, Seeley PJ. Studies of acidosis in the ischaemic heart by phosphorus nuclear magnetic resonance. *Biochem J*. 1979;184:547–554.
34. Yan GX, Kléber AG. Changes in extracellular and intracellular pH in ischemic rabbit papillary muscle. *Circ Res*. 1992;71:460–470.
35. Choi HS, Trafford AW, Orchard CH, Eisner DA. The effect of acidosis on systolic Ca^{2+} and sarcoplasmic reticulum calcium content in isolated rat ventricular myocytes. *J Physiol*. 2000;529 pt 3:661–668.
36. Wang Z, Wang T, Petrovic S, Tuo B, Riederer B, Barone S, Lorenz JN, Seidler U, Aronson PS, Soleimani M. Renal and intestinal transport defects in Slc26a6-null mice. *Am J Physiol Cell Physiol*. 2005;288:C957–C965. doi: 10.1152/ajpcell.00505.2004.
37. Flowers NC, Horan LG, Thomas JR, Tolleson WJ. The anatomic basis for high-frequency components in the electrocardiogram. *Circulation*. 1969;39:531–539.
38. Chatterjee S, Changawala N. Fragmented QRS complex: a novel marker of cardiovascular disease. *Clin Cardiol*. 2010;33:68–71. doi: 10.1002/clc.20709.
39. Pietrasik G, Zaręba W. QRS fragmentation: diagnostic and prognostic significance. *Cardiol J*. 2012;19:114–121.
40. Das MK, Maskoun W, Shen C, Michael MA, Suradi H, Desai M, Subbarao R, Bhakta D. Fragmented QRS on twelve-lead electrocardiogram predicts arrhythmic events in patients with ischemic and nonischemic cardiomyopathy. *Heart Rhythm*. 2010;7:74–80. doi: 10.1016/j.hrthm.2009.09.065.
41. Das MK, Saha C, El Masry H, Peng J, Dandamudi G, Mahenthiran J, McHenry P, Zipes DP. Fragmented QRS on a 12-lead ECG: a predictor of mortality and cardiac events in patients with coronary artery disease. *Heart Rhythm*. 2007;4:1385–1392. doi: 10.1016/j.hrthm.2007.06.024.
42. Morita H, Watanabe A, Morimoto Y, Kawada S, Tachibana M, Nakagawa K, Nishii N, Ito H. Distribution and prognostic significance of fragmented QRS in patients with brugada syndrome. *Circ Arrhythm Electrophysiol*. 2017;10. doi: 10.1161/CIRCEP.116.004765.
43. Saegusa N, Moorhouse E, Vaughan-Jones RD, Spitzer KW. Influence of pH on Ca^{2+} current and its control of electrical and Ca^{2+} signaling in ventricular myocytes. *J Gen Physiol*. 2011;138:537–559. doi: 10.1085/jgp.201110658.